

# Study on Adaptive Harmonic Extraction Approaches in Active Power Filter Applications

Alireza Fereidouni and Mohammad A.S. Masoum

**Abstract**—Active power filter (APF) has now become a mature technology for harmonic and reactive power compensations in two-wire (single phase), three-wire (three phase without neutral), and four-wire (three phase with neutral) ac power networks with nonlinear loads. This paper presents a study on three different adaptive algorithms for active power filtering applications. These algorithms are adaptive linear combiner (ADALINE), least mean square adaptive notch filter (ANF-LMS), and recursive least square adaptive notch filter (ANF-RLS). In this paper, these approaches are employed for extracting load harmonic currents. The important issues associated with adaptive methods are accuracy and prediction speed. These issues will be addressed in the paper. Simulations using MATLAB/Simulink are presented to clarify the algorithms.

**Keywords**—Harmonics, active power filters (APFs), adaptive linear combiner (ADALINE), adaptive notch filter (ANF).

## I. INTRODUCTION

Power electronic equipment usually introduces current harmonics. These current harmonics result in problems [1] such as low power factor, low efficiency, power system voltage fluctuations and communications interference. Traditional solutions for these problems are based on passive filters due to their easy design, simple structure, low cost and high efficiency. They usually consist of a bank of tuned LC filters to suppress current harmonics generated by nonlinear loads. Passive filters have many disadvantages, such as resonance, large size, fixed compensation character and possible overload. To overcome these disadvantages [2] active power filters have been presented as a current-harmonic compensator for reducing the total harmonic distortion of the current and correcting the power factor of the input source.

The main challenges associated with the implementation of APFs are device structure, generation of reference current signals and inverter control. Most APFs use voltage source inverters (VSIs) while there are also a few structures with current-source inverter (CSI) technology. In this paper also, a VSI is used for modelling the APF. There are various methods for detecting harmonic currents and calculating reference current signals, direct current control (DCC), indirect current control (ICC), instantaneous power theory (IPT) and d-q axes reference frame (SRF). In this paper, the DCC method is selected as the harmonic detection method.

Recently, ANNs have attracted much attention in different applications, including the APF. Authors in [3] computed the Fourier coefficients of the signal using ADALINE, and authors in [4] used an artificial neural network (ANN) that is trained with genetic algorithm (GA) and back propagation. Authors in [5] used a Hopfield neural network for real-time computation of frequency and harmonic content of the signal. Improved performance has been observed compared to discrete Fourier transform, fast Fourier transform, or Kalman-filtering-based approaches. An additional PI controller is used to regulate the dc-link voltage. A full “neuromimetic” strategy involving several ADALINEs has been reported by [6]. The controller can adapt for unbalance and change in working conditions. Author in [7] proposed an intelligent neural-network-based harmonic detection, which is first trained with enough data. The working model could compute the harmonic components with only one-half of the distorted wave. An ADALINE-based harmonic compensation is reported by [8]. Weights are computed online by the LMS algorithm. Authors in [9] demonstrated a 200-kVA laboratory prototype for a combined system for harmonic suppression and reactive power compensation using an optimal nonlinear PI controller, whereas a two-stage recursive least square based ADALINE is reported by [10] for harmonic measurement.

APF is a device that is connected between the non-linear load and the source. The duty of this device is to make the source current almost sinusoidal and in-phase with the source voltage in order to impose a unity power factor (PF) and improve the power quality. This means that the APF injects the harmonic and reactive currents equal but opposite of the load. In this paper, three different adaptive methods are selected to perform the harmonic extraction for APF applications. The methods are adaptive linear combiner (ADALINE), least mean square adaptive notch filter (ANF-LMS) and recursive mean square adaptive notch filter (ANF-RLS)). These approaches initially estimate the fundamental component of the load current and then subtract it from the measured current, which is the polluted load current. The outputs of the adaptive methods will be the harmonic and reactive currents.

Simulations using MATLAB/Simulink are presented to clarify the algorithms. The results reveal that the ADALINE performs slightly better than other two methods.

---

Alireza Fereidouni and Mohammad A.S. Masoum are with the Department of Electrical Engineering, Curtin University, Perth, WA, Australia ([alireza.fereidouni@curtin.edu.au](mailto:alireza.fereidouni@curtin.edu.au), [m.masoum@curtin.edu.au](mailto:m.masoum@curtin.edu.au)).

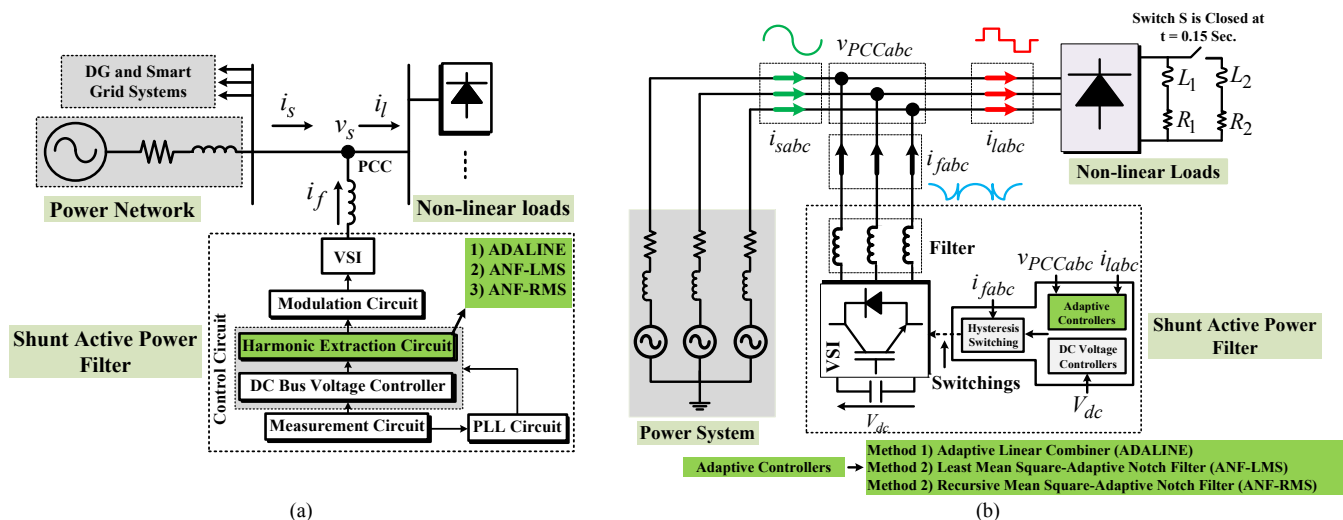


Fig. 1. APF configuration, (a) single-line diagram and (b) detailed diagram.

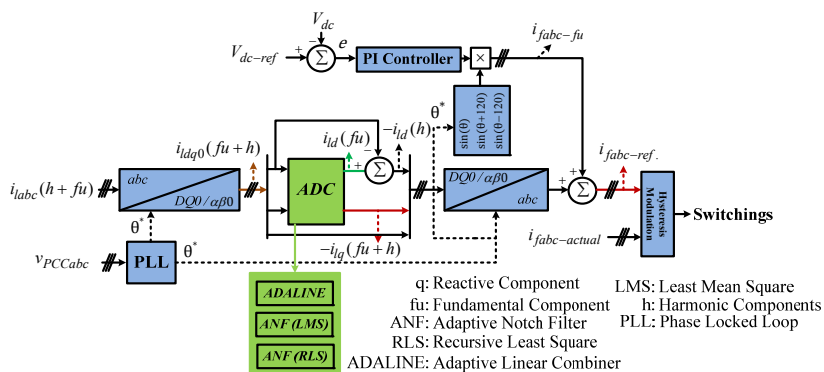


Fig. 2. Control strategy.

## II. ACTIVE POWER FILTER

### A. APF Configuration

Fig. 1 shows the basic structure of an APF. The APF is composed of a standard half-bridge three-phase VSI with a dc bus capacitor including six insulated gate bipolar transistors (IGBTs), an output well-tuned low pass filter and control system. A hysteresis based carrier-less PWM current controller is employed to achieve a fast transient APF response. The non-linear load is a dc inductive-resistive load supplied by a three-phase uncontrolled bridge. In Fig. 1,  $v_{PCCabc}$ ,  $i_{sabc}$ ,  $i_{labc}$ ,  $i_{fabc}$  and  $V_{dc}$  denote the three-phase voltages of the point of common coupling (PCC), the three-phase currents of the power system, the load, and the power converter and the DC-link voltage, respectively.

### B. Control Strategy

In this paper, the DCC approach is employed for controlling the APF meaning that the polluted load current is used for generating the reference current (shown in Fig. 2). This strategy will force the grid current ( $i_s(t)$ ) to be harmonic-free (sinusoidal) and in-phase with the PCC voltage. The total grid current is the summation of currents associated with the nonlinear load ( $i_{labc}(t)$ ) and active filter ( $i_{fabc}(t)$ ) as shown in Figs. 1 and 2:

$$i_{sabc}(t) = i_{labc}(t) + i_{fabc}(t) \quad (1)$$

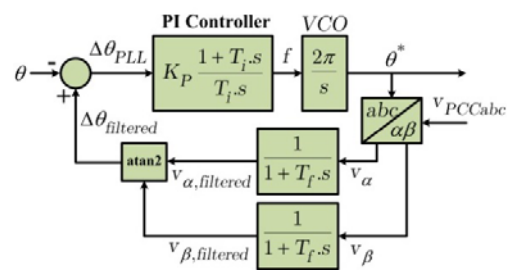
The non-linear load current includes three parts:

$$i_{labc}(t) = i_{labc-fu}(t) + \sum_{n=1}^{n_{max}} i_{labc-h_n}(t) + i_{labc-q}(t) \\ = i_{labc-fu}(t) + i_{labc-h}(t) + i_{labc-q}(t) \quad (2)$$

where  $fu$ ,  $h$ , and  $q$  represent the fundamental, harmonic, and reactive current components of the load current. The APF duty is to produce the harmonics produced by the load ( $i_{labc-h}(t)$ ) and reactive load current drawn by the load ( $i_{labc-q}(t)$ ) but in opposite sign to make the source current ( $i_{sabc}(t)$ ) almost sinusoidal and in phase with the PCC voltage (for this reason a phase-locked loop (PLL) is used (shown Fig. 3)). This means that the reference current of the APF should have opposite polarity of the harmonic ( $i_{labc-h}(t)$ ) and reactive ( $i_{labc-q}(t)$ ) load currents. To obtain the reference current, as the DCC is used, the load current is measured. In this paper, for extracting the load harmonics, three different adaptive methods are employed, which are 1) ADALINE (Fig. 4), 2) ANF-LMS (Fig. 5), and 3) ANF-RLS (Fig. 6). Therefore, these approaches first predict the fundamental component of the load current and then subtract this current by the measured current, which is the polluted load current. The output of the methods will be the harmonics and reactive currents to be generated by the VSI.

Another issue that should be taken into account in the control loop is the regulation of the dc bus voltage. To reach this goal,

Fig. 3. PLL structure.



the measured dc bus voltage ( $V_{dc}$ ) is compared with the desired voltage ( $V_{dc-ref}$ ) and the output is passed from a PI controller. The output of the controller is then summed to the reference current which yields:

$$i_{fabc-ref}(t) = -i_{labc-h}(t) - i_{labc-q}(t) + i_{fabc-fu}(t) \quad (3)$$

where  $i_{fabc-fu}(t)$  denotes the active current that the APF draws from the source in order to maintain the dc bus voltage constant.

Considering Eqs. (1-3), the source current would be:

$$i_{sabc}(t) = i_{labc}(t) + i_{fabc}(t) \\ = i_{labc-fu}(t) + i_{fabc-fu}(t) \quad (4)$$

As it can be seen from Fig. 2, two things affect the transient performance of the adaptive-control-based APF. One is the accuracy and estimation time of the adaptive methods and another one is the transient performance of the dc bus voltage controller. In this paper, the first issue is addressed by comparing the estimation results of the ADALINE, ANF-LMS, and ANF-RLS methods.

### III. ADAPTIVE APPROACHES

#### A. ADALINE Algorithm

When there are nonlinear loads in a power system, the load current and voltage waveforms are non-sinusoidal. Fourier analysis can represent a periodic waveform as sum of cosine and sine frequency components. So, the load current and the supply voltage without zero sequence components can be expressed as follows:

$$v_l = \sum_{n=1, \dots, N} [V_{n1} \cos(n\omega t) + V_{n2} \sin(n\omega t)] \quad (5)$$

$$i_l = \sum_{n=1, \dots, N} [I_{n1} \cos(n\omega t) + I_{n2} \sin(n\omega t)] \quad (6)$$

Where  $\omega$  is the waveform fundamental frequency, and  $V_{n1}$  and  $V_{n2}$  are cosine and sine frequency component amplitudes of the load voltage, and  $I_{n1}$  and  $I_{n2}$  are cosine and sine frequency component amplitudes of the load current. Two linear neurons estimate the load voltage and current components per phase. In this work, the estimation of the voltage and current frequency components are carried out by means of adaptive networks. The following model of periodical signals to be estimated is, as mentioned above:

$$f(t) = \sum_{n=1, \dots, N} [A_n \cos(n\omega t) + B_n \sin(n\omega t)] \quad (7)$$

where  $X_n$  and  $Y_n$  are the amplitude of cosine and sine components of order-n harmonic. In vectorial notation, it can be characterized as follow:

$$f(t) = \mathbf{W}^T \cdot \mathbf{X}(t) = [A_1 B_1 \dots A_N B_N] \cdot \begin{bmatrix} \cos\omega t \\ \sin\omega t \\ \dots \\ \cos N\omega t \\ \sin N\omega t \end{bmatrix} \quad (8)$$

The signals are sampled at uniform rate,  $\Delta t$ . So, time values are discrete,  $k\Delta t$  where  $k = 0, 1, 2, \dots$ . The dot product presented in Eq. (8) is carried out by one ADALINE neuron, where  $\mathbf{W}^T$  is the network weights vector. After an initial estimation of  $f(k\Delta t)$  in the case of  $k = 0$  with random weights, an adaptive algorithm updates the weights, and the

estimated signal converges to the actual one. The final network weights are the searched cosine and sine harmonic components. Fig. 4 shows the network topology and the weights update algorithm. At time  $k\Delta t$ ,  $\mathbf{X}(k\Delta t)$  is the proposed signal model and  $f_{actual}(k\Delta t)$  is the actual signal. The neurons, taking into account their weights  $\mathbf{W}(k)$ , carry out an estimation  $f_{est}(k\Delta t)$ . The error  $e(k\Delta t)$  is the difference between actual signal and its estimation. An algorithm allows to get the weights to be used in the next iteration  $\mathbf{W}(k+1)$ , which minimizes that error. After this iterative process the estimated signals adapt to the actual signals.

The weight adaptation algorithm is a modification of Widrow-Hoff (W-H) algorithm, [9], which minimizes the average square error between actual and estimated signals. It can be written as follows:

$$\mathbf{W}(k+1) = \mathbf{W}(k) + \frac{\alpha e(k) \mathbf{X}(k)}{\mathbf{X}^T(k) \mathbf{X}(k)} \quad (9)$$

Eq. (9) is the W-H rule. The scalar product  $\mathbf{X}^T(k) \mathbf{X}(k)$  is the norm of the vector  $\mathbf{X}(k)$ . So, in each iteration, weights are corrected proportionally to the error and they follow the  $\mathbf{X}(k)$  unitary direction. A modification of W-H rule can be written as follows:

$$\mathbf{W}(k+1) = \mathbf{W}(k) + \frac{\alpha e(k) \mathbf{y}(k)}{\mathbf{X}^T(k) \mathbf{y}(k)} \quad (10)$$

In Eq. (10),  $\mathbf{y}(k)$  is the  $\mathbf{X}(k)$  sign,  $\mathbf{y}(k) = \text{sgn}(\mathbf{X}(k))$ . As  $\mathbf{X}(k)$  are sinusoidal signals, if signals sign is considered, the learning rate for the weight correction will increase. The convergence-settling time decreases, though the convergence is less stable. The authors have considered an average of the signal and the signal sign. Thus, it reduces the introduced convergence problems.

$$\mathbf{y}(k) = 0.5 \text{sgn}(\mathbf{X}(k)) + 0.5 \mathbf{X}(k) \quad (11)$$

Moreover, a learning parameter is introduced to get a more stable convergence. The parameter is modified as shown in the following equation.

$$\alpha = \alpha_0 + c_1 e + c_2 \dot{e} \quad (12)$$

Thus,  $\alpha$  parameter, which depends on the linear error and its derivative, improves the algorithm convergence. Both corrections influence the convergence in opposite way; this commitment must be achieved to get stable and fast enough convergence. When the adaptive network is connected to the electrical system, the estimation convergence depends on the initial random weight chosen. Nevertheless, when the adaptive network is working online and a load change happens, the convergence does not depend on that initial choice.

#### B. Adaptive Notch filter (LMS and RLS) Algorithms

The adaptive noise cancelling strategy based on the Wiener theory has been widely utilized in many signal processing applications [11]. It can keep the system in the best operating state by continuously self-adjusting its parameters. Fig. 5 shows the basic principle of an adaptive harmonic detecting method, based on the adaptive noise cancelling theory.

In this basic configuration of adaptive filter applied to current harmonic detection,  $d(n)$  represents the load current polluted with harmonics and  $x(n)$  represents the sinusoidal waveform

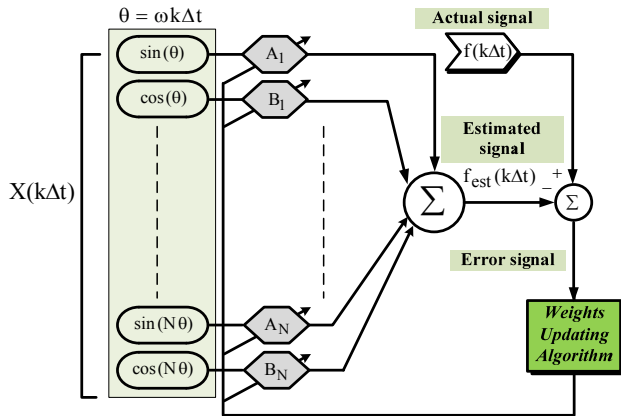


Fig. 4. Block diagram of ADALINE.

$\sin(t)$  in phase with the source voltage, generated by the PLL (shown in Fig. 3). The reference input signal  $x(n)$  is processed by the adaptive filter producing the output signal  $y(n)$  that tracks the variation in the fundamental signal of the load current. The objective of the adaptive filter is to approximate  $y(n)$ , in both amplitude and phase, to the fundamental signal  $i_1(n)$  of the load current. Therefore, the desired harmonic content  $i_h(n)$  can be directly obtained from the error signal  $e(n)$  given by subtracting  $y(n)$  from  $d(n)$ . The coefficients of the adaptive filter are adjusted using an adaptation algorithm. The adaptive notch filter is shown in Fig. 6. This structure uses two orthogonal signals as input, one for the input  $x(n)$  and the other is  $90^\circ$  phase shifted. In this way, only two coefficients are needed to be adapted. The adaptation procedure is the same as that used in the general structure of adaptive filters, and the output signal  $y(n)$  tracks the variation of the fundamental signal of the load current. Two algorithms, the LMS and the RLS, are widely used as adaptation algorithms for adaptive filters [12-19].

The recursion formula of the LMS algorithm is given by:

$$e(n) = d(n) - y(n) = d(n) - \mathbf{X}^T(n)\mathbf{W}(n) \quad (13)$$

$$\mathbf{W}(n+1) = \mathbf{W}(n) + \mu e(n)\mathbf{X}(n) \quad (14)$$

Where  $\mathbf{X}(n)$ ,  $\mathbf{W}(n)$  and  $\mu$  represent input vector, coefficient vector and step size.

The recursion formula of the LMS algorithm applied for adaptive notch filters is given by the equations:

$$w_1(n+1) = w_1(n) + \mu e(n)x(n) \quad (15)$$

$$w_2(n+1) = w_2(n) + \mu e(n)x_{90}(n) \quad (16)$$

where  $x_{90}(n)$  is  $x(n)$ ,  $90^\circ$  phase shifted. The formula of the RLS algorithm applied for adaptive notch filters, divided in five steps, is given as follows:

Step 1) Initialization  $P_{\lambda 1}(0) = 0.1$ ,  $P_{\lambda 2}(0) = 0.1$ ,  $w_1(0) = 0$ ,  $w_2(0) = 0$ ,  $\lambda = 0.9$

Step 2) Gain computation

$$k_1(n) = \frac{P_{\lambda 1}(n-1)x(n)}{\lambda + x^2(n)P_{\lambda 2}(n-1)} \quad (17)$$

$$k_2(n) = \frac{P_{\lambda 2}(n-1)x_{90}(n)}{\lambda + x_{90}^2(n)P_{\lambda 2}(n-1)} \quad (18)$$

Step 3) Output and error computation

$$y(n) = w_1(n-1)x(n) + w_2(n-1)x_{90}(n) \quad (19)$$

$$e(n) = d(n) - y(n) \quad (20)$$

Step 4) Coefficient adaptation

$$w_1(n) = w_1(n-1) + k_1(n)e(n) \quad (21)$$

$$w_2(n) = w_2(n-1) + k_2(n)e(n) \quad (22)$$

Step 5) Inverted autocorrelation coefficients

$$P_{\lambda 1}(n) = \lambda^{-1}P_{\lambda 1}(n-1) - \lambda^{-1}k_1(n)x(n)P_{\lambda 1}(n-1) \quad (23)$$

$$P_{\lambda 2}(n) = \lambda^{-1}P_{\lambda 2}(n-1) - \lambda^{-1}k_2(n)x_{90}(n)P_{\lambda 2}(n-1) \quad (24)$$

As demonstrated by the equations, in the case of the adaptive notch filter, the gain vector  $k(n)$  is transformed into gains  $k_1(n)$  and  $k_2(n)$ , calculated in Step 2. The inverse of autocorrelation matrix  $P(n)$  is transformed into two scalar values  $P_{\lambda 1}(n)$  and  $P_{\lambda 2}(n)$ , calculated in Step 5. This made the algorithm implementation simpler in terms of computational complexity. The parameter  $\lambda$  is the forgetting factor that is a positive constant close to but smaller than one. The choice of  $\lambda < 1$  results in a scheme that puts more emphasis on the recent samples of the observed values and tends to forget the past. In the literature, the adaptive notch filters are normally implemented using a PLL to generate the orthogonal input signals. These two signals are generated with Clarke transformation of the load current

$$\begin{bmatrix} I_{I0} \\ I_{I\alpha} \\ I_{I\beta} \end{bmatrix} = \sqrt{\frac{2}{3}} \begin{bmatrix} \frac{1}{\sqrt{2}} & \frac{1}{\sqrt{2}} & \frac{1}{\sqrt{2}} \\ 1 & -\frac{1}{2} & -\frac{1}{2} \\ 0 & \frac{\sqrt{3}}{2} & -\frac{\sqrt{3}}{2} \end{bmatrix} \begin{bmatrix} I_{LA} \\ I_{LB} \\ I_{LC} \end{bmatrix} \quad (25)$$

Then, the two orthogonal signals  $I_{I\alpha}$  and  $I_{I\beta}$  are filtered by a third-order Butterworth filter with a 100-Hz cutoff frequency.

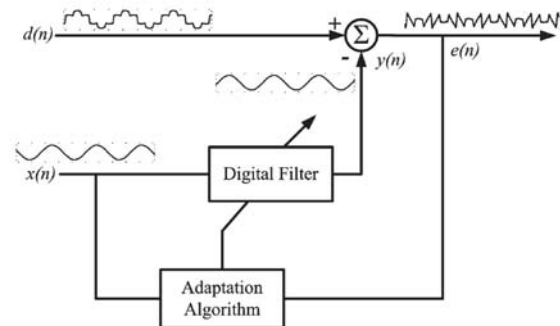


Fig. 5. Block diagram of adaptive control principle [8].

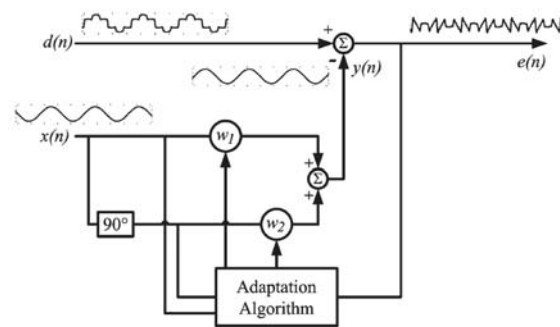


Fig. 6. Block diagram of adaptive notch filter [9].

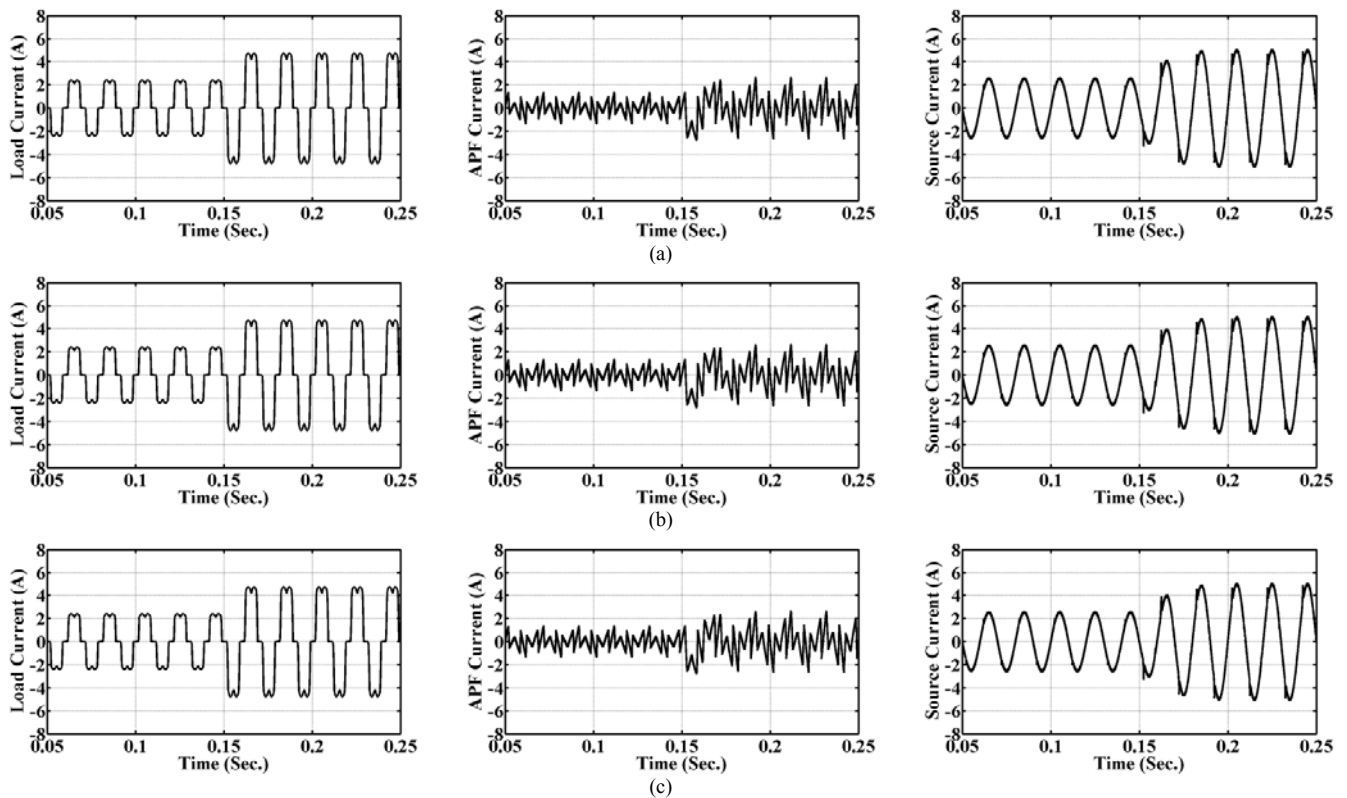


Fig. 7. APF results for (a) ADALINE, (b) ANF-LMS, and (c) ANF-RLS algorithms.

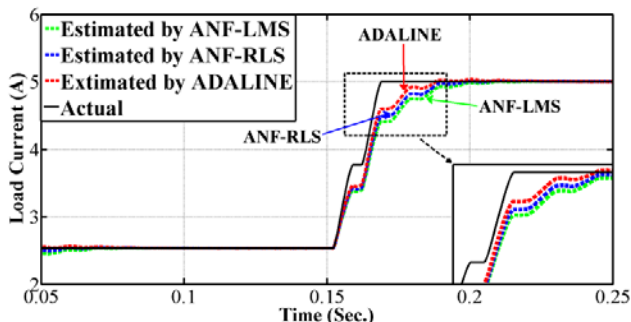


Fig. 8. Estimated fundamental load current by, (a) ADALINE, (b) ANF-LMS and (c) ANF-RLS algorithms.

#### IV. SIMULATION RESULTS

The selected APF, source and load parameters are (shown in Fig. 1)  $v_s = 415\text{ V}$ ,  $I_{fo} = 48\text{ A}$ ,  $R_f = 0.04\ \Omega$ ,  $L_f = 18\text{ mH}$ ,  $C_{dc} = 5000\ \mu\text{F}$ , and  $V_{dco} = 800\text{ V}$ ,  $R_1 = R_2 = 130\ \Omega$ , and  $L_1 = L_2 = 40\text{ mH}$ .

In this section, the power system of Fig. 1 is simulated with the control strategy of Fig. 2 in order to investigate the performance of the under studied adaptive controllers and compare them with each other. The simulation is performed for each case by closing the switch S at  $t = 0.15\text{ sec}$ . (shown in Fig. 1)). The results are shown in Figs. 7 and 8. As can be seen from Fig. 7, all algorithms show good dynamic responses when a sudden load change occurs. This means that the APF equipped with these adaptive algorithms can satisfactorily compensate the nonlinear load and make the source current sinusoidal. The fast and quick compensation of the APF improves the power quality of the

upstream power system that also leads to enhance the power system reliability. By looking closely at Fig. 8, with considering an analogous condition, it can be concluded that the ADALINE algorithm performs slightly better than other two adaptive algorithms.

#### V. CONCLUSION

This paper presents a study on three different adaptive approaches for active power filtering applications. The methods are adaptive linear combiner (ADALINE), least mean square adaptive notch filter (ANF-LMS), and recursive least square adaptive notch filter (ANF-RLS). In this paper, these approaches are employed for extracting the load harmonics currents.

The dynamic performance of the adaptive methods is measured by considering a sudden load change. Therefore, simulations are undertaken by a sudden load change. The results (Figs. 7 and 8) revealed that all adaptive algorithms work properly in the dynamic condition and moreover among which the ADALINE works slightly better than other two methods.

#### REFERENCES

- [1]. E.F. Fuchs and M.A.S. Masoum, "Power Quality in Electrical Machines and Power Systems", Elsevier, Academic Press, USA, Feb. 2008 (ISBN-13: 978-0-12-369536-9).
- [2]. S. Bhattacharya, D.M. Divan, T.M. Frank, and B. Banerjee, "Active filter system implementation," IEEE Ind. Appl. Mag., vol. 4, no. 5, pp. 47-63, Sep./Oct. 1998.
- [3]. D.M. Divan, S. Bhattacharya, and B. Banerjee, "Synchronous frame harmonic isolator using active series filter," in Proc. Eur. Power Electron. Conf., 1991, pp. 3030-3035.

- [4]. L.L. Lai, C.T. Tse, W.L. Chan, and A.T.P. So, "Real time frequency and harmonic evaluation using artificial neural network," IEEE Trans. Power Del., vol. 14, no. 1, pp. 52–59, Jan. 1999.
- [5]. L.H. Tey, P.L. So, and Y.C. Chu, "Improvement of power quality using adaptive shunt filter," IEEE Trans. Power Del., vol. 20, no. 2, pp. 1558–1568, Apr. 2005.
- [6]. D.O. Abdeslam, P. Wira, J. Merckle, D. Flieller, and Y.A. Chapuis, "A unified artificial neural network architecture for active power filters," IEEE Trans. Ind. Electron., vol. 54, no. 1, pp. 61–76, Feb. 2007.
- [7]. H.C. Lin, "Intelligent neural network-based fast power system harmonic detection," IEEE Trans. Ind. Electron., vol. 54, no. 1, pp. 43–52, Feb. 2007.
- [8]. B. Singh, V. Verma, and J. Solanki, "Neural network-based selective compensation of current quality problems in distribution system," IEEE Trans. Ind. Electron., vol. 54, no. 1, pp. 53–60, Feb. 2007.
- [9]. A. Luo, Z. Shuai, W. Zhu, and Z.J. Shen, "Combined system for harmonic suppression and reactive power compensation," IEEE Trans. Ind. Electron., vol. 56, no. 2, pp. 418–428, Feb. 2009.
- [10]. G.W. Chang, C.I. Chen, and Q.W. Liang, "A two-stage adaline for harmonics and inter-harmonics measurement," IEEE Trans. Ind. Electron., vol. 56, no. 6, pp. 2220–2228, Jun. 2009.
- [11]. B. Widrow, J.R. Glover, J.M. McCool, J. Kaunitz, C.S. Williams, R.H. Hearn, J.R. Zeidler, E. Dong, and R.C. Goodling, "Adaptive noise cancelling: Principles and applications," Proc. IEEE, vol. 63, no. 12, pp. 1692–1716, Dec. 1975.
- [12]. C.H. da Silva, V.F. da Silva, L.E. Borges da Silva, G.L. Torres, and R.R. Pereira, "DSP implementation of three-phase PLL using modified synchronous reference frame," in Proc. IEEE IECON, Taipei, Taiwan, 2007, pp. 1697–1701.
- [13]. H. Akagi, E.H. Watanabe, and M. Aredes, "Instantaneous Power Theory and Applications to Power Conditioning". Hoboken, NJ: Wiley, 2007.
- [14]. L. Asiminoaei, F. Blaabjerg, and S. Hansen, "Detection is key—Harmonic detection methods for active power filter applications," IEEE Ind. Appl. Mag., vol. 13, no. 4, pp. 22–33, Jul./Aug. 2007.
- [15]. G. Wang, H. Zhan, G. Zhang, X. Gui, and D. Xu, "Adaptive compensation method of position estimation harmonic error for EMF-based observer in sensor-less IPMSM drives," IEEE Trans. Power Electron., vol. 29, no. 6, pp. 3055–3064, 2014.
- [16]. C. Madtharad and S. Premrudeepreechacharn, "Active power filter for three-phase four-wire electric systems using neural networks," Elect. Power Syst. Res., vol. 60, no. 3, pp. 179–192, 2002.
- [17]. A. Cichocki and T. Lobos, "Artificial neural networks for real-time estimation of basic waveforms of voltages and currents," IEEE Trans. Power Syst., vol. 9, no. 2, pp. 612–618, May 1994.
- [18]. F.J. Alcántara, P. Salmerón, and J. Prieto, "A new technique for unbalance current and voltage measurement with neural networks," in Proc. CD\_ROM 9th Eur. Conf.
- [19]. H.C. Wood, and N.G. Johnson, "Kalman filtering applied to power system measurements for relaying," IEEE Trans. Power Apparatus Syst., vol. 104, pp. 3565–3573, 1985.

**Alireza Fereidouni** received his B.S. and M.S. degrees in Electrical Engineering from University of Mazandaran, Babolsar, Iran in 2009 and Amirkabir University of Technology, Tehran, Iran in 2012, respectively. He is presently working towards a Ph.D. degree in Electrical Engineering and Computer Department at Curtin University, Perth, Australia. He was awarded a Curtin International Postgraduate Research Scholarship (CIPRS) in 2013.

**Mohammad A.S. Masoum** received his B.S., M.S. and Ph.D. degrees in Electrical and Computer Engineering in 1983, 1985, and 1991, respectively, from the University of Colorado, USA. Currently, he is a Professor in the Electrical and Computer Engineering Department, Curtin University, Australia. Dr. Masoum is the co-author of *Power Quality in Power Systems and Electrical Machines* (Elsevier, 2008) and *Power Conversion of Renewable Energy Systems* (Springer, 2011). He is a senior member of IEEE.